

# Regulatory Mechanisms that Mediate Tenascin C-Dependent Inhibition of Oligodendrocyte Precursor Differentiation

Tim Czopka,<sup>1,2</sup> Alexander von Holst,<sup>1,2</sup> Charles ffrench-Constant,<sup>3</sup> and Andreas Faissner<sup>1,2</sup>

<sup>1</sup>Department of Cell Morphology and Molecular Neurobiology, and <sup>2</sup>International Graduate School of Neuroscience, Ruhr-University, D-44780 Bochum, Germany, and <sup>3</sup>Medical Research Council Centre for Regenerative Medicine and Multiple Sclerosis Society Translational Research Centre, Centre for Inflammation Research, The Queen's Medical Research Institute, University of Edinburgh, Edinburgh EH16 4TJ, United Kingdom

Here, we present mechanisms for the inhibition of oligodendrocyte precursor cell (OPC) differentiation, a biological function of neural extracellular matrix (ECM). The differentiation of oligodendrocytes is orchestrated by a complex set of stimuli. In the present study, we investigated the signaling pathway elicited by the ECM glycoprotein tenascin C (Tnc). Tnc substrates inhibit myelin basic protein (MBP) expression of cultured rat oligodendrocytes, and, conversely, we found that the emergence of MBP expression is accelerated in forebrains of Tnc-deficient mice. Mechanistically, Tnc interfered with phosphorylation of Akt, which in turn reduced MBP expression. At the cell surface, Tnc associates with lipid rafts in oligodendrocyte membranes, together with the cell adhesion molecule contactin (Cntn1) and the Src family kinase (SFK) Fyn. Depletion of Cntn1 in OPCs by small interfering RNAs (siRNAs) abolished the Tnc-dependent inhibition of oligodendrocyte differentiation, while Tnc exposure impeded the activation of the tyrosine kinase Fyn by Cntn1. Concomitant with oligodendrocyte differentiation, Tnc antagonized the expression of the signaling adaptor and RNA-binding molecule Sam68. siRNA-mediated knockdown or overexpression of Sam68 delayed or accelerated oligodendrocyte differentiation, respectively. Inhibition of oligodendrocyte differentiation with the SFK inhibitor PP2 could be rescued by Sam68 overexpression, which may indicate a regulatory role for Sam68 downstream of Fyn. Our study therefore uncovers the first signaling pathways that underlie Tnc-induced, ECM-dependent maintenance of the immature state of OPCs.

## Introduction

During development, oligodendrocyte precursor cells (OPCs) migrate throughout the brain and gradually differentiate at appropriate places to myelinate target axons. We are interested in how the extracellular matrix (ECM) affects the differentiation of oligodendrocytes. Tenascin C (Tnc) is an ECM glycoprotein that is abundantly expressed in the developing brain and vanishes as the organism matures (Joester and Faissner, 2001). We have previously shown that OPCs proliferate less but migrate faster within the optic nerves of Tnc-deficient mice (Garcion et al., 2001) and that cultured OPCs from Tnc-deficient mice display higher maturation rates (Garwood et al., 2004). Tnc is a functional component of astroglial ECM and interferes with myelin basic protein (MBP) expression and myelin sheet formation (Czopka et al., 2009b). The differential activation of small GTPases of the RhoA family proved responsible for the Tnc-induced effects on membrane formation (Czopka et al., 2009b). However, the GTPases

had no effect on MBP expression, and the molecular mechanisms that prevent differentiation are therefore not understood.

Several Tnc receptors and their downstream signaling pathways are implicated in oligodendrocyte development. Tnc-dependent proliferation of OPCs depends on  $\alpha_v\beta_3$  integrin (Garcion et al., 2001). Tnc also interacts with the cell adhesion molecule (CAM) contactin (Cntn1) (Zacharias et al., 1999; Rigato et al., 2002), which in turn associates with the Src family kinase (SFK) Fyn in lipid rafts (Kramer et al., 1999). Lipid raft formation is necessary for integrin-dependent signaling via phosphatidylinositol-3 kinase (PI3K) to mediate oligodendrocyte survival (Decker and ffrench-Constant, 2004). The Fyn tyrosine kinase is a key effector of oligodendrocyte differentiation and myelination because Fyn-deficient animals are hypomyelinated (Umemori et al., 1994; Sperber et al., 2001) and their oligodendrocytes display defective branching and membrane formation (Osterhout et al., 1999). Moreover, Fyn activity regulates expression and alternative splicing of MBP, involving the RNA-binding molecule quaking I (Lu et al., 2005). The quaking/STAR family (Lukong and Richard, 2003) also includes Sam68 that functions as a signaling transducer for Fyn-mediated migration in fibroblasts (Huot et al., 2009) and as a phosphorylation-dependent splicing regulator for *Bcl-X* and *CD44* in different cell lines (Matter et al., 2002; Paronetto et al., 2007). As yet, Sam68 has not been implicated in oligodendrocyte development but is specifically downregulated by Tnc in neural stem cells (Moritz et al., 2008) and hence represents a plausible Tnc target in oligodendrocytes.

Received Oct. 6, 2009; revised July 12, 2010; accepted July 22, 2010.

This work was supported by the German Ministry of Education, Research and Technology (Grant BMBF 01GN0503, to A.F.) and by the Protein Research Department of the Ruhr-University. T.C. was supported through the Ph.D. program of the International Graduate School of Neuroscience and the Research School at the Ruhr-University supported by the Deutsche Forschungsgemeinschaft (GSC 98/1). C.ff.-C. was supported by the Biotechnology and Biological Sciences Research Council. We thank Dr. H. König (Forschungszentrum, Karlsruhe, Germany) for providing the Sam68 full-length plasmid.

Correspondence should be addressed to Andreas Faissner, Department of Cell Morphology and Molecular Neurobiology, Ruhr-University Bochum, Universitätsstrasse 150, NDEF 05/594, D-44780 Bochum, Germany. E-mail: Andreas.Faissner@ruhr-uni-bochum.de.

DOI:10.1523/JNEUROSCI.4957-09.2010

Copyright © 2010 the authors 0270-6474/10/3012310-13\$15.00/0

In the present study, we have therefore analyzed these signaling pathway(s) to determine how Tnc reduces MBP expression in oligodendrocytes. We show that the effect of Tnc on MBP expression requires Cntn1- as well as Tnc-dependent interference with Fyn and Akt activation. Moreover, we show that the signaling adaptor and RNA-binding molecule Sam68 is expressed in oligodendrocytes and downregulated in response to Tnc and other inhibitors of differentiation. Knockdown of Sam68 delayed MBP expression, whereas Sam68 overexpression favored differentiation. We propose, therefore, that Tnc regulates these pathways to control oligodendrocyte differentiation.

## Materials and Methods

**Animals.** Tnc mutant mice were previously generated (Forsberg et al., 1996). Animals were bred in a SV129 background and used for the *in vivo* analysis of oligodendrocyte differentiation. Wild-type (WT) and knockout littermates of both sexes from heterozygote crosses were identified by PCR as described previously (Talts et al., 1999). For cell culture experiments, we used CD rat pups that were obtained from the Charles River Laboratories.

**Antibodies and other reagents.** We used the following mouse monoclonal antibodies: O4 (Sommer and Schachner, 1981); MBP (Sigma; DM1A against  $\alpha$ -tubulin (Sigma); Cntn1 (BD Bioscience); and Fyn, ErbB4, fibroblast growth factor (FGF) receptor 2, and Sam68 (all Santa Cruz Biotechnology). The following rabbit polyclonal antibodies were used: KAF14 against Tnc (Faissner and Kruse, 1990); neural CAM (NCAM) (Keilhauer et al., 1985); Cntn1 (Rigato et al., 2002); epidermal growth factor receptor (EGFR), Fyn, platelet-derived growth factor (PDGF) receptor  $\alpha$ , and Sam68 (all Santa Cruz Biotechnology); phospho-Src family kinase-Y418 and Y529 (both Biosource/Invitrogen); pErk1/2, pAkt-Ser473, pAktThr308, panAkt (against all three Akt isoforms) (all Cell Signaling Technology). The polyclonal antibodies against laminin and fibronectin were generated by immunization of rabbits with Engelbreth-Holm-Swarm sarcoma-purified laminin and human fibronectin, respectively (data not shown). We noticed that the mouse anti-Sam68 antibody consistently yielded a double band in Western blots, whereas the rabbit anti-Sam68 revealed only one band. At present, we do not know whether the second band represents an isoform (as predicted from the bioinformatic database ensemble), a posttranslational modification (e.g., phosphorylation), or simply a contaminating cross-reactivity to an unrelated gene product.

For immunological detection methods, all biotinylated, CY2-, CY3-, and horseradish peroxidase-coupled secondary antibodies were obtained from Dianova, alkaline phosphatase-coupled antibodies from Roche, and Alexa Fluor 350 from Invitrogen. We obtained laminin-1 from Invitrogen and human fibronectin from TEBU. Human recombinant PDGF-AA, FGF-2, and the active domain of NRG-1 and EGF are from PeptoTech. Insulin was from Sigma. We used small interfering RNA (siRNA) duplexes against rat Cntn1 and nontarget control RNA as published (Laursen et al., 2009). The siRNA duplexes against rat Sam68 were obtained from Invitrogen and composed of the following nucleotides: 5'-GAAGAUUCUUGGACCACAAtt-3' (sense), 5'-UUGUGUCCAA-GAAUCUUCc-3' (antisense). The Sam68 full-length plasmid was a kind gift from Dr. H. König, Forschungszentrum Karlsruhe, Karlsruhe, Germany (Matter et al., 2002). LY294002 was obtained from Cell Signaling Technology, PP2 was from Calbiochem/Merck, and wortmannin was from Biomol.

**Cell culture.** OPCs were harvested by the "shake-off" method of McCarthy and deVellis (1980) from rat cortical cultures with modifications as described (Milner and French-Constant, 1994). For immunocytochemical staining, purified OPCs were plated on 12 mm glass coverslips coated with 10  $\mu$ g/ml poly-ornithine (P-Orn) (Sigma) followed by coating with different ECM molecules at 10  $\mu$ g/ml each for at least 1 h at 37°C. OPCs were cultured in DMEM containing 1% N2-supplement, 1% penicillin/streptomycin (all from Invitrogen) and 100  $\mu$ g/ml BSA V (AppliChem) at 37°C, 7.5% CO<sub>2</sub>. For immunoblotting, OPCs were cultured in six-well (Greiner Bio-One) or 10 cm (Nunc) dishes coated as above. When high cell quantities were needed, OPCs were expanded in the presence of 10 ng/ml PDGF-AA and FGF-2 for up to 3 d before induction of differentiation. Differentiation was induced by growth-factor with-

drawal and the addition of 400 ng/ml tri-iodothyronin (T3; Sigma) and 1% FCS (Invitrogen). LY294002, PP2, and wortmannin were added at time points and concentrations as indicated in the figures. If not specified, 5  $\mu$ M LY294002 and 2  $\mu$ M PP2 were used.

**Immunocytochemistry.** Immunocytochemical stainings were performed as previously described (von Holst et al., 2006; Czopka et al., 2009a).

**Immunoprecipitation.** For immunoprecipitation of Fyn, we used 2–3  $\times$  10<sup>6</sup> OPCs per experimental condition. The cells were treated with PBS, Tnc, or laminin-2 (Invitrogen) for 2 h by adding it into the culture medium, or by exposure to P-Orn or Tnc-coated culture dishes for 2 d (for the densitometry). The cells were lysed in modified RIPA buffer (50 mM Tris pH 7.4, 150 mM NaCl, 1% NP-40, 0.25% Na-deoxycholate, 1 mM EDTA, 1 mM Na<sub>3</sub>VO<sub>4</sub>, 1 mM NaF) and collected with a cell scraper. The lysates were cleared by centrifugation for 10 min at 10,000  $\times$  g. Fyn was immunoprecipitated from the cleared lysate with 1  $\mu$ g mouse anti-Fyn antibody and 20  $\mu$ l Protein A/G Agarose (50% slurry) (Santa Cruz Biotechnology) for 4 h at 4°C on a rotating wheel. The precipitate was washed twice with modified RIPA buffer by centrifugation for 5 min at 500  $\times$  g. Finally, the pellet was boiled at 95°C and subsequently processed for SDS-PAGE analysis.

**Immunoblotting.** Cell lysates were subjected to SDS-PAGE and subsequently blotted to polyvinylidene fluoride membranes (Roth). The membranes were blocked with 5% low-fat milk powder (local food store) in TBST for 1 h at room temperature (RT), followed by the incubation with primary antibodies in blocking solution overnight at 4°C. After incubation with the appropriate horseradish peroxidase-conjugated secondary antibodies for 1 h at RT, signals were detected by enhanced chemoluminescence (Pierce).

**Tissue preparation and in situ hybridization.** Brains were fixed overnight at 4°C with 4% paraformaldehyde and subsequently cryoprotected in 30% DEPC-treated sucrose for an additional 24 h at 4°C. The tissue was embedded in tissue-freezing medium (Jung) and frozen on dry ice. Sectioning was performed on a cryostat (Leica). *In situ* hybridizations were performed following a published protocol (Pringle et al., 1996) on 16  $\mu$ m frontal cryosections. The RNA probes were produced with the FITC-RNA labeling kit according to the manufacturers instructions (Roche); *Mbp* (nucleotides 719–1696 in the reference sequence NM\_001025259, covering all isoforms) and *Sox10* (nucleotides 541–1620 in the reference sequence XM\_985075).

**RNA isolation, cDNA synthesis, and amplification.** Total RNA was isolated from 3  $\times$  10<sup>5</sup> oligodendrocytes per experimental condition with the RNeasy Mini Kit (Qiagen) according to the manufacturer's instructions. cDNA was transcribed with the first-strand cDNA synthesis kit (MBI; Fermentas) according to the manufacturers instructions. For PCR amplifications, the following primers were used: *Mbp*\_3'UTR\_for: 5'-GGACTGCAGGAGTCTCTGG-3', *Mbp*\_3'UTR\_rev: 5'-GTGC-CAGTGTGGGTCTCTTT-3'; *Cntn1*\_for: 5'-AGAACCCATGCCT-ACCACAG-3', *Cntn1*\_rev: 5'-AAACTGGGTTTTGGTGCAG-3'; *Cntn2*\_for: 5'-GATTAAGCAGATGGTCCCTTTGG-3', *Cntn2*\_rev: 5'-GAAGGGAAGAGAGTAGCGTTCA-3';  $\beta$ -Actin\_for: 5'-TATGC-CAACACAGTGCTGTCTGGTGG-3',  $\beta$ -Actin\_rev: 5'-AGAAGCA-CTTGCGGTGCACGATGG-3'. Primers for the amplification of glyceraldehyde 3-phosphate dehydrogenase (GAPDH) were from MBI Fermentas and included in the cDNA synthesis kit.

**Sucrose density gradient centrifugation.** Lipid rafts were isolated from 3  $\times$  10<sup>6</sup> oligodendrocytes as described (Kramer et al., 1999).

**Transfection of primary oligodendrocytes.** The cultivation protocols for transfections of primary rat OPCs with individual siRNA and/or plasmid DNA are depicted schematically in the respective figures. In general, freshly isolated OPCs were expanded in PDGF- and FGF-2-containing medium for 2 d. Then, the cells were removed from the culture dishes by brief trypsinization with 0.25% Trypsin/EDTA (Invitrogen) at 37°C. The trypsin activity was stopped through addition of an equal volume of Ovomucoid [1 mg/ml soybean trypsin inhibitor (Sigma), 50  $\mu$ g/ml BSA, and 40  $\mu$ g/ml DNaseI (Worthington) in L-15 medium (Sigma)]. OPCs were collected by centrifugation for 5 min at 200  $\times$  g. For each experimental condition, 4–5  $\times$  10<sup>6</sup> cells were transfected with the Amaxa Rat Oligodendrocyte Nucleofection Kit (Lonza) according to the manufac-

turer's instructions. For the knockdown experiments, 200 pmol siRNA duplexes against *Cntn1*, *Sam68*, or control RNA were cotransfected with 0.5  $\mu$ g pMaxGFP (Lonza) or pCX-myrVenus (Rhee et al., 2006) using electroporation program O-17. This represents a 1:5 ratio of green fluorescent protein (GFP) DNA to siRNA (in  $\mu$ g). For overexpression experiments, we used 0.5  $\mu$ g of pcDNA3.1 (Invitrogen) containing full-length *Sam68* (Matter et al., 2002).

**Isolation of *Tnc*.** *Tnc* protein was isolated by immunoaffinity chromatography as described previously (Faissner and Kruse, 1990; Czopka et al., 2009b).

**Documentation and data analysis.** Immunoblots were scanned, and the mean optical density of the bands was measured using the ImageJ software (<http://rsb.info.nih.gov/ij/>). Photomicrographs of immunocytochemical stainings were taken on an Axioplan2 microscope with the Plan-NEOFLUAR objectives 2.5 $\times$ /0.075, 10 $\times$ /0.30, 20 $\times$ /0.50, 40 $\times$ /0.75 or 63 $\times$ /1.4 Oil (all Zeiss). Digital photomicrographs were captured with the AxioCam HRC camera and the AxioVision 4.5 software (both Zeiss). For quantifications of immunopositive cells, a minimum of 200 Hoechst-positive nuclei or 50 transfected cells were counted in at least three independent experiments for each antibody and condition. Successfully transfected cells were identified either by GFP stain or the clear overrepresentation of the respective gene product. For the densitometric analysis of *Sam68* expression levels in cultured oligodendrocytes, photomicrographs (1300  $\times$  1030 pixels) of *Sam68* stainings were taken with the 40 $\times$  objective. For the analysis of the *Sam68* signal, we plotted circles (26  $\times$  26 pixels) over the nuclear *Sam68* signals and measured their mean optical density with ImageJ software. For the quantification of *in situ* hybridizations, *Sox10*- or *Mbp*-reactive somata that were detectable in the cortical gray matter between corpus callosum and pial surface were counted. At least three tissue slices were analyzed per individual animal. All data are expressed as the mean  $\pm$  SD or SEM, as indicated in the figure legends. Statistical significance was assessed using the two-tailed Student's *t* test, and the *p* values are given as \**p*  $\leq$  0.05, \*\**p*  $\leq$  0.01, and \*\*\**p*  $\leq$  0.001 in the figures and/or legends.

## Results

***Tnc* inhibits oligodendrocyte differentiation in culture, and *Tnc*-deficient mice show altered oligodendrocyte maturation**  
Previous studies examining *Tnc*, laminins, and hyaluronan have demonstrated the importance of the ECM for proper oligodendrocyte development and function (Garcion et al., 2001; Colognato et al., 2002; Back et al., 2005). To investigate the impact of *Tnc* on oligodendrocytes using a convenient cell culture assay, culture dishes were coated with poly-ornithine alone or in a combination with 10  $\mu$ g/ml fibronectin, laminin-1, or *Tnc*. Subsequently, rat OPCs were plated and allowed to differentiate on these substrates (Fig. 1). Under all experimental conditions, none of the substrates significantly affected the fraction of the total cell population that were O4-positive immature or mature oligodendrocytes (Fig. 1*A, B*). However, the proportion of terminally differentiated MBP-positive oligodendrocytes was reduced nearly

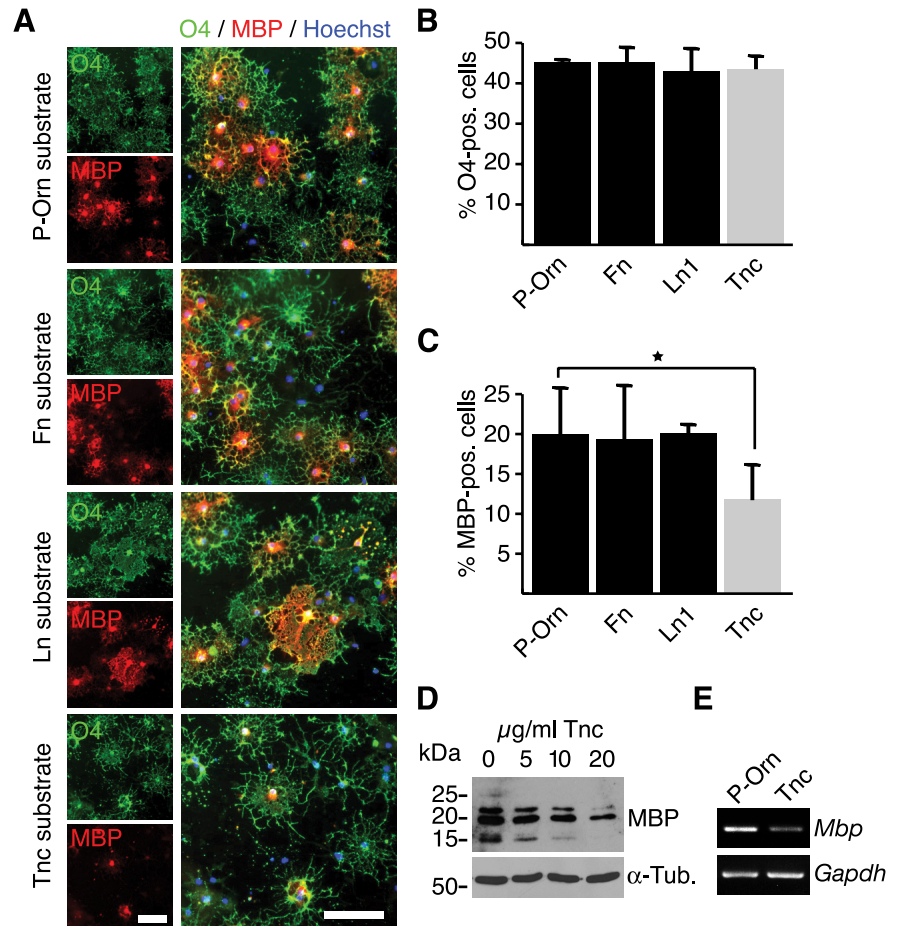


**Figure 1.** *Tnc* substrates inhibit MBP expression in cultured rat oligodendrocytes. **A**, Oligodendrocytes cultivated on P-Orn or various ECM substrates and labeled by immunocytochemistry for O4 and MBP are shown. Nuclei are marked in blue (Hoechst stain). **B**, The fraction of O4-positive immature oligodendrocytes was unaffected by the substrate conditions, including *Tnc* ( $n = 5$ ). Data are expressed as mean  $\pm$  SD. **C**, The fraction of MBP-positive mature oligodendrocytes is reduced on *Tnc*, but not on laminin (Ln1) or Fibronectin (Fn) (\* $p < 0.05$ ,  $n = 5$ ). Data are expressed as mean  $\pm$  SD. **D**, Immunoblots for MBP of oligodendrocytes cultured on increasing amounts of *Tnc* substrate reveal a dose-dependent reduction in MBP expression. Tubulin served as loading control ( $\alpha$ -Tub). **E**, RT-PCR analysis of RNA extracts showing that *Mbp* mRNA levels were selectively reduced after cultivation on a *Tnc* substrate. Scale bar, 100  $\mu$ m.

twofold on *Tnc* (19.9%  $\pm$  5.7 on P-Orn vs 11.8%  $\pm$  4.1 on *Tnc*;  $p = 0.03$ ;  $n = 5$  Fig. 1*A, C*). The other substrates tested had no effect on the proportion of MBP-positive cells. All MBP-expressing cells still coexpressed O4 (Fig. 1*A*), indicating that oligodendrocytes are maintained in an immature O4-positive/MBP-negative stage. The *Tnc*-induced repression in MBP expression was dose dependent, as when increasing amounts of *Tnc* were used for coating a progressive diminution of MBP expression occurred (Fig. 1*D*). This was also reflected at the mRNA level, as RT-PCR analysis amplified less *Mbp* mRNA when the cells were cultured on a *Tnc*-coated dish (Fig. 1*E*).

As *Tnc* strongly repressed MBP expression in culture, one would predict effects of *Tnc* ablation *in vivo*. To test this, oligodendrocyte maturation in the forebrains of *Tnc* mutant mice was analyzed and compared with wild-type littermates. *Tnc* expression is most prominent before myelination starts (supplemental Fig. 1*C*, available at [www.jneurosci.org](http://www.jneurosci.org) as supplemental material), so we focused on these early stages. *In situ* hybridization revealed that at postnatal day 10 (P10), the onset of oligodendrocyte differentiation and myelination in the forebrain, more *Mbp*-expressing cells were detectable in the gray matter of *Tnc* mutants compared with controls (Fig. 2). The *in situ* hybridizations con-

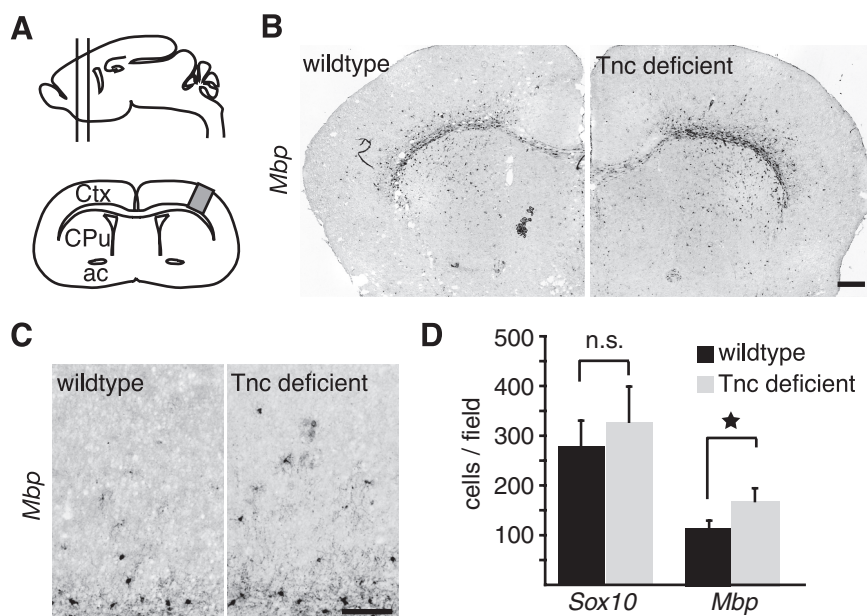


**Figure 2.** Accelerated *Mbp* expression in forebrains of *Tnc* mutant mice. **A**, Schematic drawing of the forebrain region studied. The analysis was confined to the boxed cortical region on frontal sections (lower drawing) that contained the anterior commissure as a landmark. **B, C**, Photomicrographs of *in situ* hybridizations for *Mbp* in P10 wild-type and knock-out littermates are shown. The pictures show stronger reactivity for *Mbp* in the *Tnc*-deficient brain. **D**, The quantification of cells that express *Mbp* or *Sox10* in the dorsal cortex between corpus callosum and pial surface shows that the fraction of *Mbp*-positive cells is significantly higher in the *Tnc* knock-outs ( $*p = 0.03$ ;  $n = 5$ ). The quantification of *Sox10*-positive cells did not show a significant increase ( $p = 0.6$ ;  $n = 4$ ). Data in are expressed as mean  $\pm$  SEM. Scale bars, 200  $\mu$ m. Ctx, Cortex; CPu, caudate–putamen; ac, anterior commissure; n.s., not significant.

sistently developed stronger *Mbp* signals in the *Tnc*-deficient tissue (Fig. 2*B*), and we detected more *Mbp*-positive cells in the cortical gray matter dorsal of the corpus callosum (Fig. 2*C*). Increased numbers were confirmed by quantifying the *Mbp*-expressing cells in the cortical gray matter between corpus callosum and pial surface. Here, significantly more cells were labeled in the *Tnc*-deficient tissue using the *Mbp* riboprobe ( $110 \pm 13$  cells/slide in WT vs  $160 \pm 24$  cells/slide in KO;  $p = 0.03$ ;  $n = 4$ ) (Fig. 2*D*).

Our earlier reports had shown that the migration rate of OPCs is elevated in *Tnc*<sup>-/-</sup> optic nerves (Garcion et al., 2001). To rule out the possibility that augmented *Mbp* expression in the cortex is a result of increased OPC migration rather than of premature differentiation, we additionally quantified the number of cells expressing *Sox10*, a transcription factor also expressed at earlier stages of oligodendrocyte development (Stolt et al., 2002). Any increased OPC migration into the cortex would be expected to result in increased numbers of *Sox10*-expressing cells. However, no significant differences between WT and *Tnc*-deficient tissue were detectable ( $278 \pm 51$  cells/slide in WT vs  $328 \pm 70$  in KO; not significant;  $n = 4$ ) (Fig. 2*D*). This indicates that OPC differentiation is accelerated in *Tnc* mutant mice. However, this difference was transient, as *Mbp* expression appeared comparable in wild-type and mutants at later stages of forebrain development (supplemental Fig. 1, available at [www.jneurosci.org](http://www.jneurosci.org) as supplemental material). This could be explained by the developmental disappearance of endogenous *Tnc* expression during the second postnatal week of mouse forebrain development (Czopka et al., 2009b).

### Tnc signaling is independent of PDGF but involves reduced phosphorylation of Akt

Previous studies on the role of the ECM in oligodendrocyte behavior have revealed that the ECM molecule vitronectin activates

$\alpha_v\beta_3$  integrins and so sensitizes cultured OPCs to physiological amounts of the growth factor PDGF (Baron et al., 2002). This means that, in the presence of appropriate ECM, low amounts of endogenous growth factors might be sufficient to keep OPCs in an immature, MBP-negative state. To test whether the effect of the *Tnc* substrate on MBP expression can be explained by modified sensitivity to growth factors, OPCs were cultivated on *Tnc* or control substrates and simultaneously exposed to different concentrations of PDGF. Immunocytochemical staining for MBP showed that the number of MBP-positive oligodendrocytes on P-Orn was the same at PDGF concentrations of 0–1 ng/ml (Fig. 3*A–C*) and that, regardless of PDGF concentration used, the number of MBP-expressing cells was always lower on the *Tnc* substrate. This indicates that *Tnc* does not amplify the response to low amounts of PDGF, because were this the case at high PDGF concentrations the numbers of MBP-positive cells would be the same with or without *Tnc* (Fig. 3*A–C*). As another way to confirm that the *Tnc* effect is independent of PDGF, low-dose growth factor treatment (i.e., 1 ng/ml)

was used to investigate whether PDGF treatment or *Tnc* exposure affected the phosphorylation profile of downstream signaling molecules in a comparable way. Immunoblotting for the phosphorylation of Erk1/2 and Akt, two major signaling effectors downstream of receptor tyrosine kinases, showed distinct differences when comparing treatment with *Tnc* and with PDGF (Fig. 3*D*), and *Tnc* exposure weakened the phosphorylation of Akt whether or not PDGF was added (Fig. 3*D*). This attenuation proved statistically significant when phospho-Akt blots were measured densitometrically ( $p = 0.04$ ;  $n = 4$ ). Similarly, after treatment with low doses of neuregulin or EGF instead of PDGF, and also after only short-term application of different growth factors, phospho-Akt was consistently reduced in the presence of *Tnc* (supplemental Fig. 2, available at [www.jneurosci.org](http://www.jneurosci.org) as supplemental material). Therefore, we conclude that the *Tnc*-mediated reduction of MBP expression is independent of the growth factor conditions, but is associated with mitigation of Akt activity.

Akt is an important intermediate in the PI3K signaling pathway, which plays a crucial role in cell survival (Flores et al., 2000; Hutchinson et al., 2001) and myelination (Flores et al., 2008). For this reason, a potential influence of the *Tnc* substrate on oligodendrocyte survival was investigated. Immunocytochemical staining for activated caspase-3 showed only low levels of apoptosis in all conditions. These were not significantly increased when the cells were grown on substrates coated with 5 or 10  $\mu$ g/ml *Tnc* ( $2.5\% \pm 1.5$  on P-Orn;  $7.0 \pm 11.1$  at 5  $\mu$ g/ml *Tnc*,  $p = 0.5$ ;  $5.0 \pm 3.2$  at 10  $\mu$ g/ml *Tnc*,  $p = 0.2$ ;  $n = 4$ ) (Fig. 3*E*).

To elucidate whether this change in phosphorylation of Akt might be functionally involved in the differentiation of oligodendrocytes, we perturbed PI3K signaling (the upstream regulator of Akt) using the pharmacological inhibitors wortmannin or LY294002. As these two components have different half-life times in water (not shown), they were applied at different intervals to

the cultures to ensure constant perturbation of PI3K activity (Fig. 4A). Triple immunostaining for PDGFR $\alpha$ , O4, and MBP showed that exposure to 5  $\mu$ M LY294002 reduced the fraction of terminally differentiated MBP-expressing cells ( $20.9 \pm 7.9\%$  control vs  $8.9 \pm 0.9\%$  LY294002,  $n = 3$ ), but not that of O4-positive immature oligodendrocytes ( $56.3 \pm 8.9\%$  control vs  $71.1 \pm 6.6\%$  LY294002,  $n = 3$ ) and PDGFR $\alpha$ -expressing precursors ( $22.6 \pm 10.5\%$  control vs  $19.9 \pm 6.8\%$  LY294002,  $n = 3$ ) (Fig. 4B,C). The LY294002-induced reduction in MBP expression was statistically significant and dose dependent ( $27.7 \pm 6.9\%$  control;  $7.4 \pm 3.1\%$  at 5  $\mu$ M LY294002,  $p < 0.001$ ;  $1.3 \pm 2.5\%$  at 10  $\mu$ M LY294002,  $p < 0.001$ ;  $n = 4$ ) (Fig. 4D), and is clearly seen by immunoblotting (Fig. 4E). Wortmannin was used as an independent inhibitor of PI3K signaling and confirmed the observations obtained with LY294002 (Fig. 4F). To rule out that the reduction in MBP expression was mainly a result of the death of differentiated cells, we assessed the number of apoptotic cells by activated caspase-3 staining. Here, a significantly increased number of dying cells was only seen when the concentration of LY294002 was 10  $\mu$ M ( $2.5 \pm 1.5\%$  in DMSO control;  $5.1 \pm 4.9\%$  at 5  $\mu$ M LY294002,  $p = 0.35$ ;  $11.4 \pm 8.8\%$  at 10  $\mu$ M LY294002,  $p = 0.09$ ;  $n = 4$ ) (Fig. 4G,H). At concentrations of  $\geq 20 \mu$ M, LY294002 proved highly apoptotic (data not shown). However, in both control and 5  $\mu$ M LY294002 condition, the majority of activated caspase-3 expressing cells were O4-positive immature oligodendrocytes ( $82.7 \pm 12.1\%$  in DMSO control;  $83.6 \pm 8.0\%$  at 5  $\mu$ M LY294002;  $n = 3$ ) (Fig. 4I) and not the MBP-positive population ( $3.8 \pm 3.3\%$  in DMSO control;  $4.8 \pm 5.7\%$  at 5  $\mu$ M LY294002;  $n = 3$ ) (Fig. 4I). This shows that the reduction in MBP expression is not a result of selective cell death in the terminally differentiated cell fraction. Together, these results therefore support the conclusion that Tnc-mediated inhibition of MBP expression involves a reduced phosphorylation of Akt that inhibits oligodendrocyte differentiation, so extending recent findings demonstrating the importance of the PI3K/Akt/mTOR pathway for oligodendrocyte differentiation (Narayanan et al., 2009; Tyler et al., 2009).

### Tnc associates with lipid rafts and forms a functional signaling complex with Cntn1 and Fyn

Cntn1 is one of the cell surface receptors for Tnc (Falk et al., 2002; Rigato et al., 2002) and regulates oligodendrocyte maturation (Hu et al., 2003; White et al., 2008; Laursen et al., 2009). The interaction between Tnc and Cntn1 has been studied in several experimental systems including coprecipitation from brain extracts (Rigato et al., 2002), aggregation assays in cell lines (Zacharias et al., 1999), and cell-free aggregation assays (Rigato et al.,

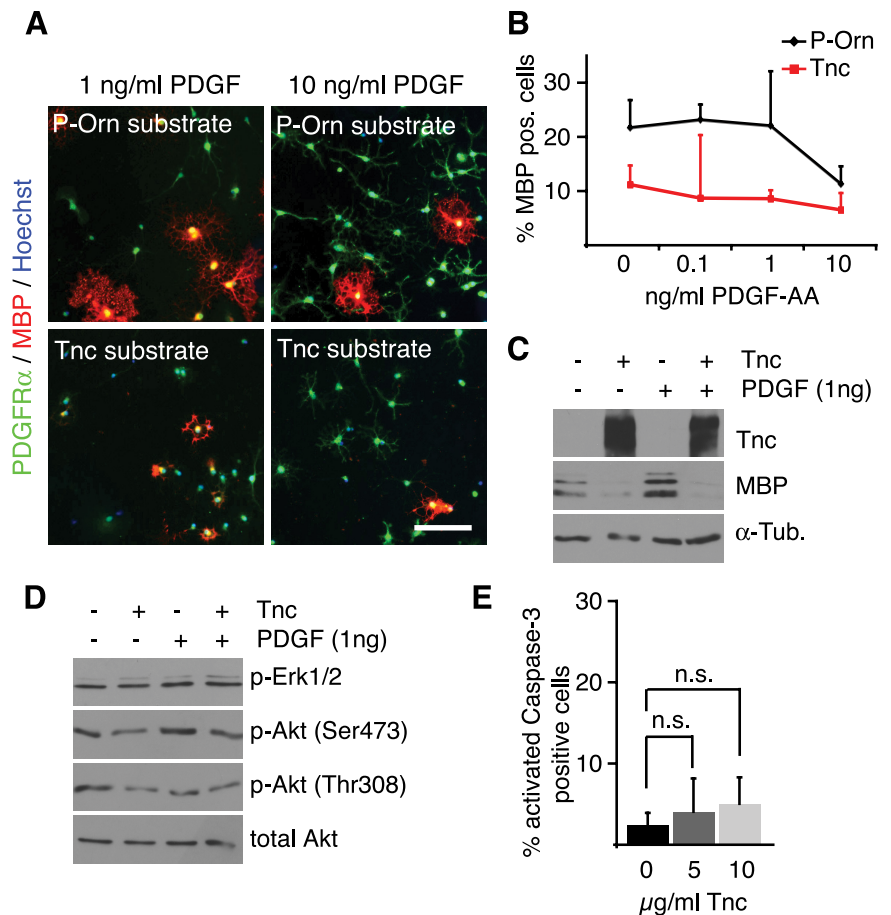


**Figure 3.** Tnc does not amplify the response to PDGF but reduces phosphorylation of Akt. **A**, Immunocytochemical stainings for PDGFR $\alpha$  and MBP in oligodendrocytes cultured on P-Orn or Tnc substrates in the presence of different PDGF concentrations. Note that increased numbers of PDGFR $\alpha$ -positive OPCs are only observable when PDGF was present at 10 ng/ml, regardless of the culture substrate. **B**, Quantification of MBP-expressing cells using the methods described in **A**. PDGF only reduced the number of MBP-expressing cells at 10 ng/ml, but not at lower concentrations on P-Orn. On Tnc, MBP-expressing cells are less numerous in the absence of PDGF, and PDGF did not further reduce MBP expression arguing against any amplification effect between Tnc and PDGF on differentiation signaling. **C**, Immunoblotting of cultures grown on P-Orn or Tnc in the presence or absence of 1 ng/ml PDGF shows that the addition of PDGF has no effect on the Tnc-mediated inhibition of MBP expression. **D**, Immunoblotting for phospho-Erk1/2 and phospho-Akt in cultures treated as indicated shows that Tnc reduced the phosphorylation of Akt independently of the presence or absence of PDGF. In contrast, phospho-Erk1/2 remained unaffected by Tnc. **E**, Quantification of caspase-3-expressing cells shows that cultivation on a Tnc substrate does not significantly increase cell death ( $p = 0.5$  at 5  $\mu$ g/ml Tnc,  $p = 0.2$  at 10  $\mu$ g/ml Tnc;  $n = 4$ ). Data are expressed as mean  $\pm$  SD. Scale bar, 200  $\mu$ m; n.s., Not significant.

2002). In the present study, we were also able to document that Tnc protein coprecipitated from mixed glial cultures after immunoprecipitation with a Cntn1-specific antibody, but not when an nonspecific mouse IgG was used (Fig. 5A). This indicates that the interaction between Tnc and Cntn1 is not limited to neurons. Hence, Cntn1 seemed a promising candidate to mediate Tnc signaling in OPC differentiation. To test this, Cntn1 siRNA duplexes were introduced into primary OPCs by nucleofection (Fig. 5B). This resulted in a substantial knockdown of the Cntn1 protein and its mRNA, whereas related adhesion molecules of the Ig superfamily such as Cntn2 (TAG-1) and NCAM were not affected (Fig. 5C,D). To test whether Cntn1 is involved in the Tnc-mediated repression of oligodendrocyte differentiation, transfected cells were cultured either on a P-Orn or Tnc substrate. Successfully transfected OPCs were identified by cotransfection with a GFP-coding plasmid. The transfection efficiency with a GFP-coding plasmid was  $\sim 40\%$  (supplemental Fig. 7A, available at [www.jneurosci.org](http://www.jneurosci.org) as supplemental material). Given that siRNA was transfected in molar excess and would be expected to

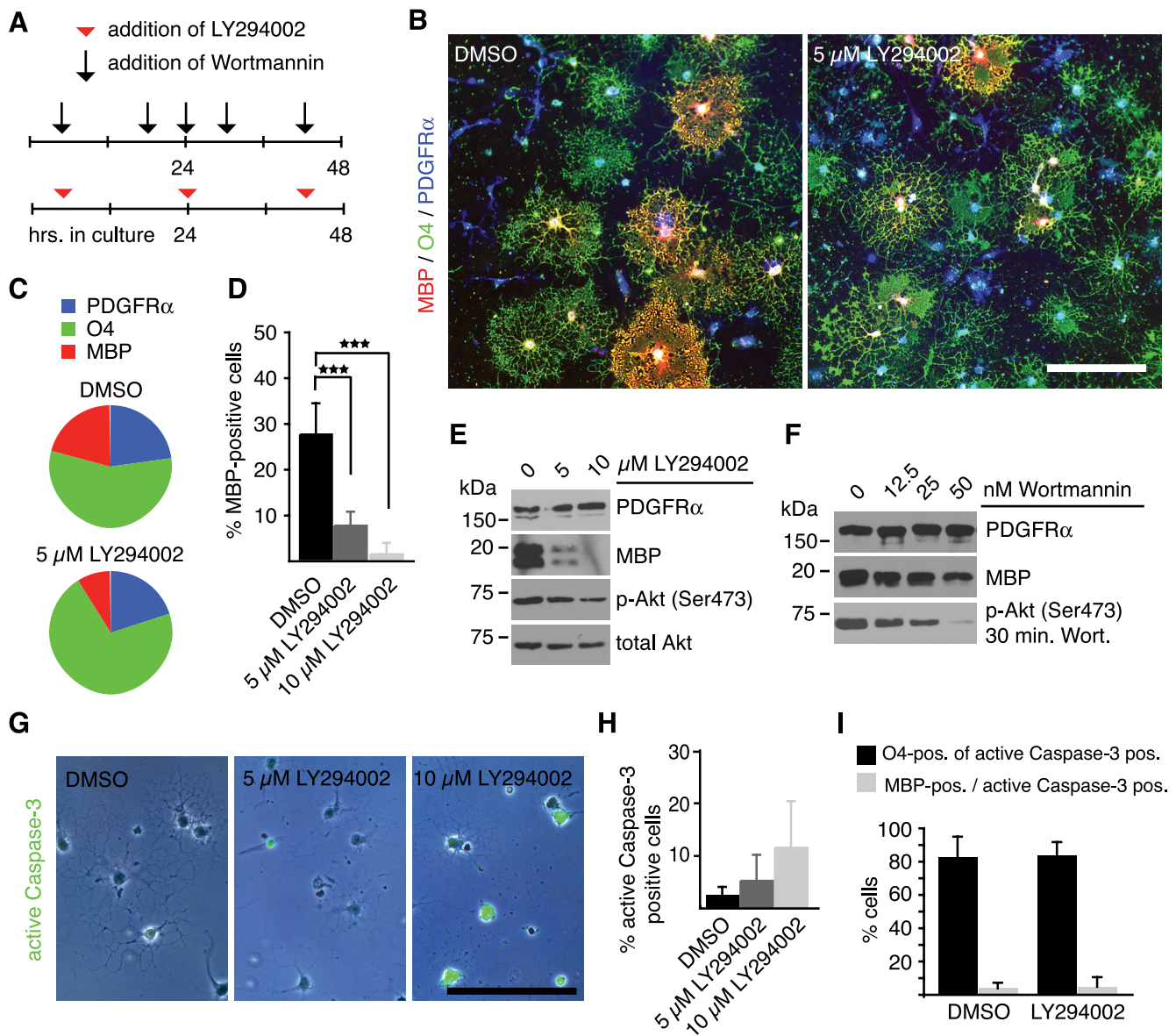


**Figure 4.** Impaired PI3K signaling reduces MBP expression in oligodendrocytes. **A**, Oligodendrocytes were cultured for two d in the presence or absence of the PI3K inhibitors wortmannin or LY294002 as indicated. **B**, Representative photomicrographs of control- and LY294002-treated oligodendrocyte cultures triple stained for PDGFR $\alpha$ , O4, and MBP. **C**, The pie chart shows that LY294002 treatment reduces the MBP-positive but not the O4- or PDGFR $\alpha$ -expressing cell fraction ( $n = 3$ ). **D**, The diagram reveals the significant reduction of MBP-expressing cells after treatment with 5 and 10  $\mu$ M LY294002 (\*\*\* $p$  < 0.001;  $n = 4$ ). **E**, Immunoblotting confirms reduced MBP expression resulting from LY294002 treatment. Note that levels of phosphorylated Akt were reduced but not completely suppressed. Total Akt serves as a loading control. **F**, Immunoblotting shows that wortmannin treatment similarly reduces MBP in a dose-dependent fashion ( $p = 0.3$  at 5  $\mu$ M;  $p = 0.09$  at 10  $\mu$ M;  $n = 4$ ). Data are expressed as mean  $\pm$  SD. **G**, **H**, Caspase-3 staining and subsequent quantification reveals that LY294002 increased the number of apoptotic cells in a dose-dependent fashion ( $p = 0.3$  at 5  $\mu$ M;  $p = 0.09$  at 10  $\mu$ M;  $n = 4$ ). Data are expressed as mean  $\pm$  SD. **I**, The quantification shows that caspase-3-expressing cells are present in equal proportions in the O4- and MBP-expressing cell fraction in control and LY294002-treated cultures ( $n = 3$ ). Data are expressed as mean  $\pm$  SD. Scale bars, 150  $\mu$ m.

enter cells more easily due its comparably small size, we assumed that each GFP-expressing cell was also cotransfected with siRNA. When the RNA control sequence was introduced, many GFP-positive cells on the Tnc substrate did not coexpress MBP (Fig. 5E). In contrast, most GFP-positive cells on the Tnc substrate coexpressed MBP when the Cntn1 siRNA knockdown sequence was cotransfected (Fig. 5E). Quantification showed that the Tnc-mediated reduction in MBP expression was apparent upon transfection with a scrambled control sequence ( $69.6 \pm 6.4$  on P-Orn vs  $46.2 \pm 13.9$  on Tnc,  $p = 0.02$ ,  $n = 4$ ) (Fig. 5F) but was reversed by the knockdown of Cntn1 so that almost similar numbers of MBP-expressing cells developed on the P-Orn and Tnc substrate ( $85.7 \pm 5.7$  on P-Orn vs  $82.9 \pm 6.8$  on Tnc,  $p = 0.5$ ,  $n = 4$ ) (Fig.

5F). We thus conclude that the cell surface adhesion protein Cntn1 is necessary to mediate Tnc-dependent repression of oligodendrocyte differentiation.

Molecules that actively participate in signaling often associate in lipid rafts, which are characterized by their detergent insolubility at 4°C (for review, see Gielen et al., 2006). By virtue of its glycosylphosphatidylinositol (GPI) link to the plasma membrane, Cntn1 is almost exclusively confined to lipid rafts. Because Cntn1 was required for effective Tnc signaling as shown above, we reasoned that other transducers of Tnc signaling may also associate with the raft. To further investigate this, lipid rafts were isolated from cultured oligodendrocytes by sucrose density gradient ultracentrifugation. The low sucrose raft fraction was

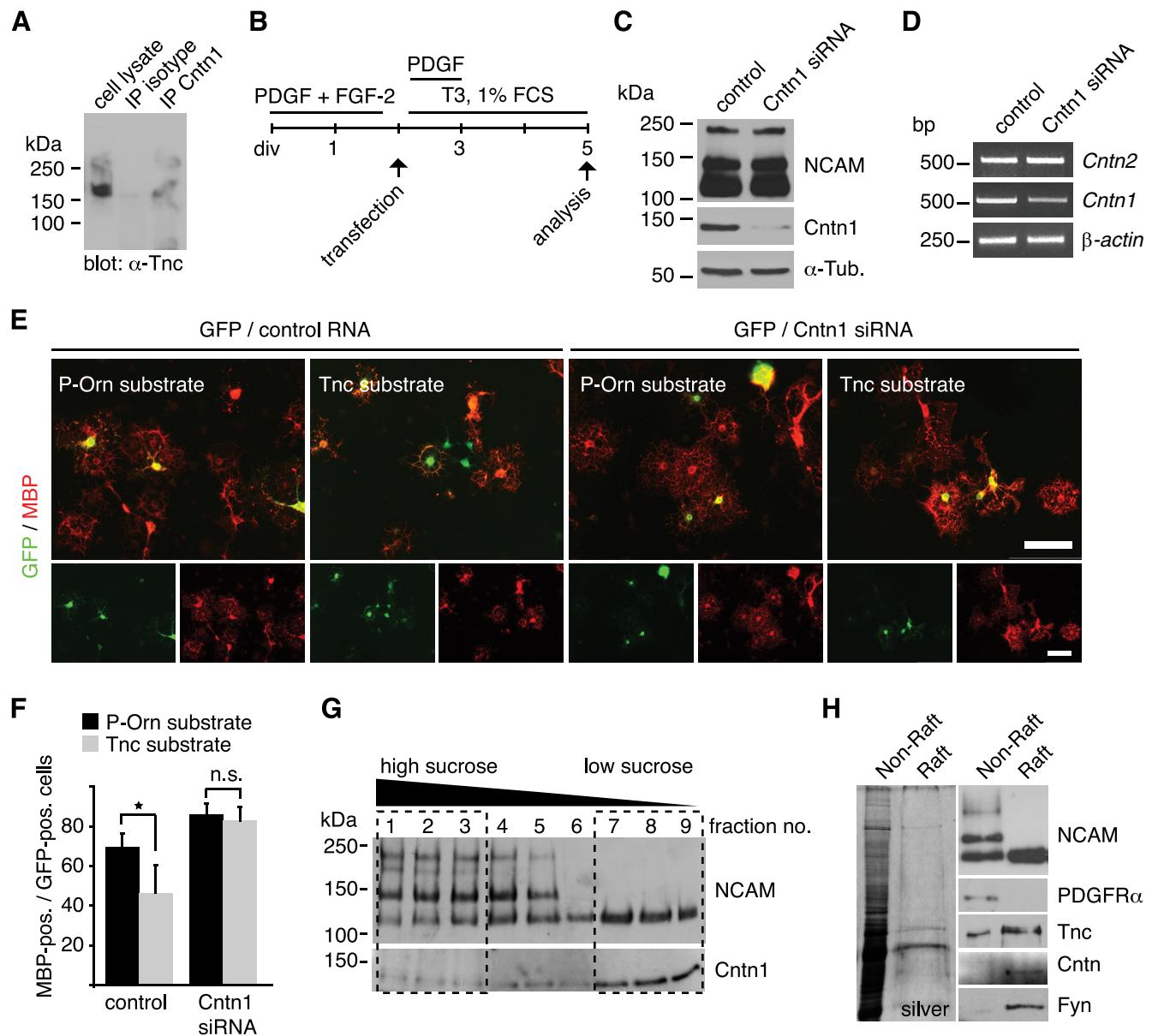


**Figure 5.** Tnc-mediated inhibition of MBP expression depends on Cntn1 and both molecules are present in lipid rafts. **A**, Western blotting for Tnc shows that Tnc coprecipitates when Cntn1 was immunoprecipitated from mixed glial cultures. This is not the case when a nonspecific mouse IgG was used. **B**, Schematic drawing of the cultivation protocol for OPC transfection with siRNA duplexes against Cntn1. “PDGF + FGF-2” refers to the OPC expansion phase, “T3 + 1%FCS” means differentiating culture conditions. **C**, Immunoblotting confirms successful knockdown of Cntn1 protein while NCAM is not affected. Tubulin served as loading control ( $\alpha$ -Tub). **D**, PCR analysis after Cntn1 knockdown reveals a reduction of *Cntn1*, but not *Cntn2* mRNA levels. *Actin* served as loading control. **E**, **F**, Photomicrographs of OPCs that were cultivated on P-Orn or Tnc substrates after cotransfection with GFP and siRNAs and immunostained for MBP. The quantification displays the proportion of transfected (GFP-positive) cells that coexpressed MBP on control P-Orn or Tnc substrates. The number of MBP-expressing GFP-positive cells is significantly reduced on Tnc after control transfection. This was abolished after Cntn1 knockdown ( $n = 4$ ,  $*p \leq 0.05$ ). n.s., Not significant. Data are expressed as mean  $\pm$  SD. **G**, Immunoblotting for NCAM and Cntn1 after sucrose density gradient ultracentrifugation. The 140 and 180 kDa forms of NCAM containing fractions 1–3 were designated to be the “nonraft” fraction, whereas fractions 7–9 were selected as “raft” fraction due to the accumulation of Cntn1 and the 120 kDa NCAM isoform. **H**, The silver-stained SDS gel shows that the raft fraction contains considerably less protein than the nonraft fraction. Nevertheless, immunoblotting reveals that Tnc is prominently detectable in the raft fraction, together with NCAM 120, Cntn1, and Fyn but not the PDGFR $\alpha$ . Scale bar, 100  $\mu$ m.

traced by the accumulation of the GPI-anchored molecules Cntn1 and the 120 kDa isoform of NCAM, and its composition was compared with the high sucrose non-raft fraction (Fig. 5*G,H*; supplemental Fig. 3, available at [www.jneurosci.org](http://www.jneurosci.org) as supplemental material). As reported earlier (Kappler et al., 2002), Tnc was prominently, although not exclusively, detectable in the raft fraction (Fig. 5*H*; supplemental Fig. 3, available at [www.jneurosci.org](http://www.jneurosci.org) as supplemental material). The Src kinase Fyn, an established signaling partner of Cntn1 localized to the cytosolic side of the plasma membrane and involved in oligodendrocyte

differentiation (Kramer et al., 1999; Osterhout et al., 1999; Colongato et al., 2004), was also present in the raft fraction (Fig. 5*H*; supplemental Fig. 3, available at [www.jneurosci.org](http://www.jneurosci.org) as supplemental material). In contrast to these molecules, many other cell surface receptors and intracellular signaling partners did not show raft accumulation, including Akt (supplemental Fig. 3, available at [www.jneurosci.org](http://www.jneurosci.org) as supplemental material).

In keeping with the concentration of a signaling complex within membrane subdomains, a punctate distribution of Tnc across the plasma membrane was observed by immunostaining

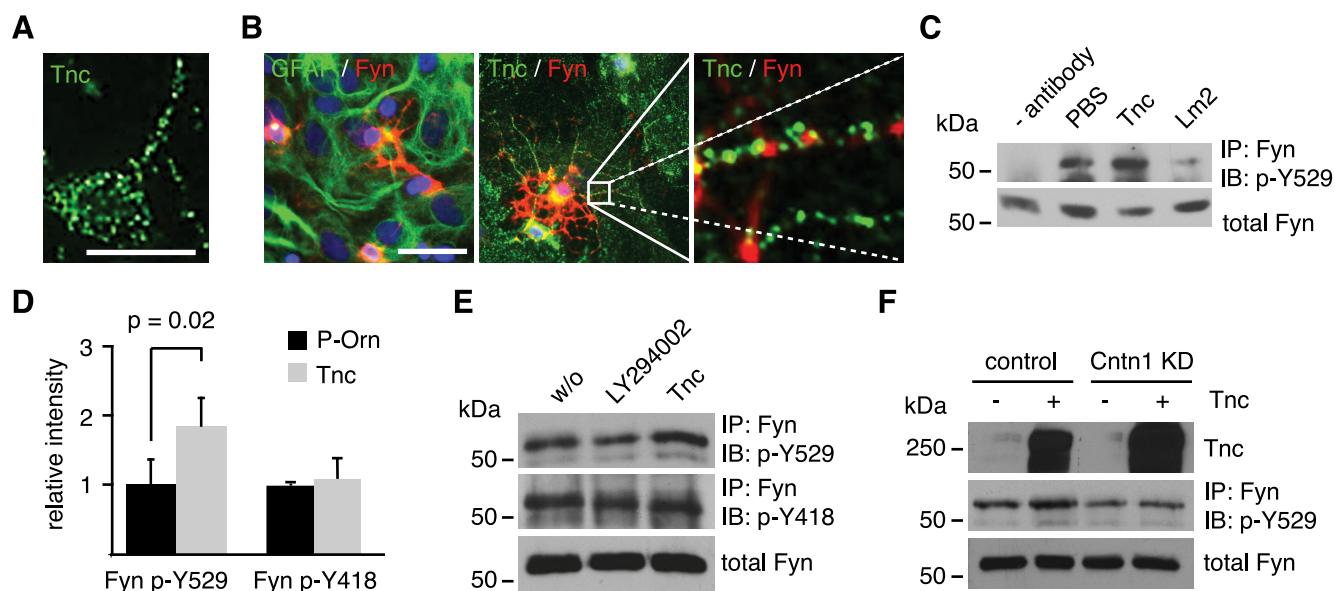


**Figure 6.** Tnc reduces Fyn activity in a Cntn1-dependent manner. *A*, Immunostaining for Tnc in OPCs results in a punctate pattern across the membrane. *B*, Immunostaining of Fyn-expressing oligodendrocytes on GFAP-positive, Tnc-expressing astrocytes shows that Tnc and Fyn partially colocalize in oligodendrocyte processes (right). *C*, Immunoprecipitation of Fyn from oligodendrocytes exposed to PBS or Tnc for 2 h and subsequent blotted for the phosphorylated Y529 residue yielded increased signals when the cells were exposed to Tnc. Note that phosphorylated Y529 is reduced by laminin-2. *D*, Densitometry of phospho-Y529 levels confirms a twofold increase on Tnc ( $p = 0.02$ ;  $n = 3$ ), whereas phospho-Y418 is not altered ( $p = 0.45$ ;  $n = 5$ ). The data are expressed as mean  $\pm$  SD. *E*, Immunoprecipitation of Fyn from oligodendrocytes shows that LY294002 treatment does not change the phosphorylated Y529 levels. Also note that phosphorylation of the catalytic Y418 is unaltered by LY294002 or Tnc. *F*, Immunoprecipitation of Fyn demonstrates that the Tnc-induced increase in phospho-Y529 is abolished upon knockdown of Cntn1. Scale bars: *A*, 25  $\mu$ m; *B*, 50  $\mu$ m.

for Tnc in OPCs (Fig. 6*A*). This was also true when oligodendrocytes were cocultured with astrocytes that provide a physiological source for Tnc-containing neural ECM. Double-labeling experiments for Tnc and the Fyn kinase showed both to be present in a punctate staining pattern along the oligodendrocyte processes (Fig. 6*B*). Eighty-two of 365 Fyn-positive puncta on 18 individual cells were also immunoreactive for Tnc, showing that both molecules partially colocalized, which is consistent with the presence of a signaling complex within membrane subdomains.

To investigate how Tnc signaling might control the activity of Fyn, we examined phosphorylation at the regulatory residue tyrosine 531 (Y531) of the rat Fyn kinase that negatively regulates its kinase activity. In a first set of experiments, we stimulated oligodendrocytes with different ECM molecules that were added to the culture medium for 2 h. When Fyn was then immunoprecipitated and probed for phosphorylated Y531 (which was detected with an anti SFK-phospho-Y529 antibody), the addition of Tnc was found to increase phosphorylation compared with PBS-treated cells (Fig. 6*C*). In contrast to Tnc, exposure to laminin-2 (which favors differentiation) reduced phospho-Y529 levels (Fig. 6*C*), as previously reported (Colognato et al., 2004). Next, we measured the degree of Fyn phosphorylation for cells grown on P-Orn or Tnc substrates, and showed a statistically significant increase in phospho-Y529 levels on Tnc (Fig. 6*D*) ( $p = 0.021$ ,  $n = 3$ ). We also observed that phosphorylation of the catalytic tyrosine Y420 of rat Fyn (which was detected with anti SFK-phospho-Y418 antibody) was not significantly altered by Tnc treatment (Fig. 6*D,E*) ( $p = 0.45$ ;  $n = 5$ ). LY294002, which also inhibits differentiation, affected neither phospho-Y418 nor-Y529 levels (Fig. 6*E*; supplemental Fig. 4*A,B*, available at www.jneurosci.org as supplemental material). This argues for a direct effect of Tnc on Fyn. It also argues that PI3K-mediated signaling represents a pathway either separate from or downstream of Fyn, with the latter interpretation supported by the observation that

the SFK inhibitor PP2 blocks both Src/Fyn and Akt activation (supplemental Fig. 4*C*, available at www.jneurosci.org as supplemental material). Importantly, we could no longer detect increased phospho-Y529 levels in response to Tnc after Cntn1 knockdown (Fig. 6*F*), indicating that the signaling from Tnc to Fyn depends on Cntn1.

### Sam68 is expressed in oligodendrocytes and regulates MBP expression in a Tnc-dependent manner

In an independent induction gene-trap approach, we have previously searched for Tnc-regulated target genes in neural stem/progenitor cells to obtain new insights as to how Tnc mechanistically affects cellular behavior. In this screen, the signaling adapter and RNA-binding molecule Sam68 emerged as a gene that is repressed in response to Tnc (Moritz et al., 2008). Sam68 is related to quaking proteins, which are potent regulators of myelin gene translation (Larocque and Richard, 2005). Moreover, Sam68 acts downstream of Fyn (Lang et al., 1999) and has also been described as initiator of PI3K signaling (Sanchez-Margalet and Najib, 1999), both of which are involved in Tnc-mediated inhibition of MBP expression, as we have shown above. We therefore investigated whether Sam68 might be involved in the Tnc-dependent regulation of MBP expression. First, the expression of Sam68 was analyzed in the oligodendrocyte lineage. Double-immunocytochemistry revealed that Sam68 was detectable in A2B5-expressing OPCs, O4-positive immature oligodendrocytes as well as in terminally differentiated MBP-expressing oligodendrocytes (supplemental Fig. 5*A*, available at www.jneurosci.org as supplemental material). Sam68 was prominent in the cell nuclei and also in the processes of oligodendrocytes (Fig. 7*A*). This cytosolic localization of Sam68 has previously been reported in other cells (Grange et al., 2004; Huot et al., 2009). The expression of Sam68 within all stages of oligodendrocyte development was confirmed by immunoblotting, which also



showed that total Sam68 levels increase with differentiation (Fig. 7B). The densitometric analysis of Sam68 immunoreactivity revealed that MBP-positive oligodendrocytes show ~50% higher Sam68 expression rates than A2B5-expressing OPCs ( $1.0 \pm 0.1$  in A2B5-positive cells vs  $1.5 \pm 0.4$  in MBP-positive;  $p = 0.02$ ,  $n = 5$ ). In contrast to this, when oligodendrocytes were exposed to purified Tnc, a consistent reduction of Sam68 protein level was observed when compared with untreated cells (Fig. 7C). In this regard, the oligodendrocytes behaved similarly to neural stem cells (Moritz et al., 2008). Other inhibitors of MBP expression such as the SFK inhibitor PP2 (supplemental Fig. 6, available at [www.jneurosci.org](http://www.jneurosci.org) as supplemental material) and the PI3K inhibitor LY294002 also led to reduced Sam68 protein levels (Fig. 7D–F), indicating that other pathways also regulate the levels of Sam68 protein.

To investigate whether Sam68 has an instructive role in oligodendrocyte differentiation, we used siRNA to knock down Sam68 in primary rat OPCs (Fig. 8A). To identify successfully transfected cells, the siRNA was cotransfected with a Venus-coding plasmid, a variant of the yellow fluorescent protein (Nagai et al., 2002). As already argued for the Cntn1 siRNA (see above), each cell labeled with fluorescent protein expression is most probably cotransfected with siRNA, although exceptions cannot formally be excluded. However, immunoblotting of whole-cell lysates confirmed a reduction in Sam68 levels after transfection with Sam68 siRNAs (Fig. 8B; supplemental Fig. 7D, available at [www.jneurosci.org](http://www.jneurosci.org) as supplemental material) and densitometric quantification of Sam68 immunoreactivity in cultured oligodendrocytes showed ~60% knock-down efficiency ( $0.91 \pm 0.1$  in control vs  $0.41 \pm 0.06$ ,  $p < 0.001$ ,  $n = 4$ ) (supplemental Fig. 7B, C, available at [www.jneurosci.org](http://www.jneurosci.org) as supplemental material). Interestingly, we also observed reduced MBP levels in the Sam68 knockdown cultures by immunoblotting 3 d after transfection (Fig. 8B). This observation was supported by immunocytochemistry. Here, significantly fewer transfected cells coexpressed MBP after knockdown ( $47.5\% \pm 4.9$  in control vs  $28.8\% \pm 9.2$  after Sam68 siRNA,  $p = 0.01$ ,  $n = 4$ ) (Fig. 8C). Conversely, when heterologous Sam68 was overexpressed in primary OPCs (Fig. 8D, E; supplemental Fig. 7E, available at [www.jneurosci.org](http://www.jneurosci.org) as supplemental material), higher MBP levels were detected by immunoblotting of total cell lysates 2 d after transfection (Fig. 8E), and by immunocytochemistry a significantly increased proportion of cells coexpressed MBP ( $32.9\% \pm 7.6$  in control vs  $49.6 \pm 7.7$  after Sam68 overexpression;  $p = 0.03$ ,  $n = 5$ ). Together, these results show that appropriate levels of Sam68 are necessary for efficient oligodendrocyte differentiation.

Sam68 also functions as a signal transducer as it is both a substrate of Fyn (Lang et al., 1999; Paronetto et al., 2007) and an

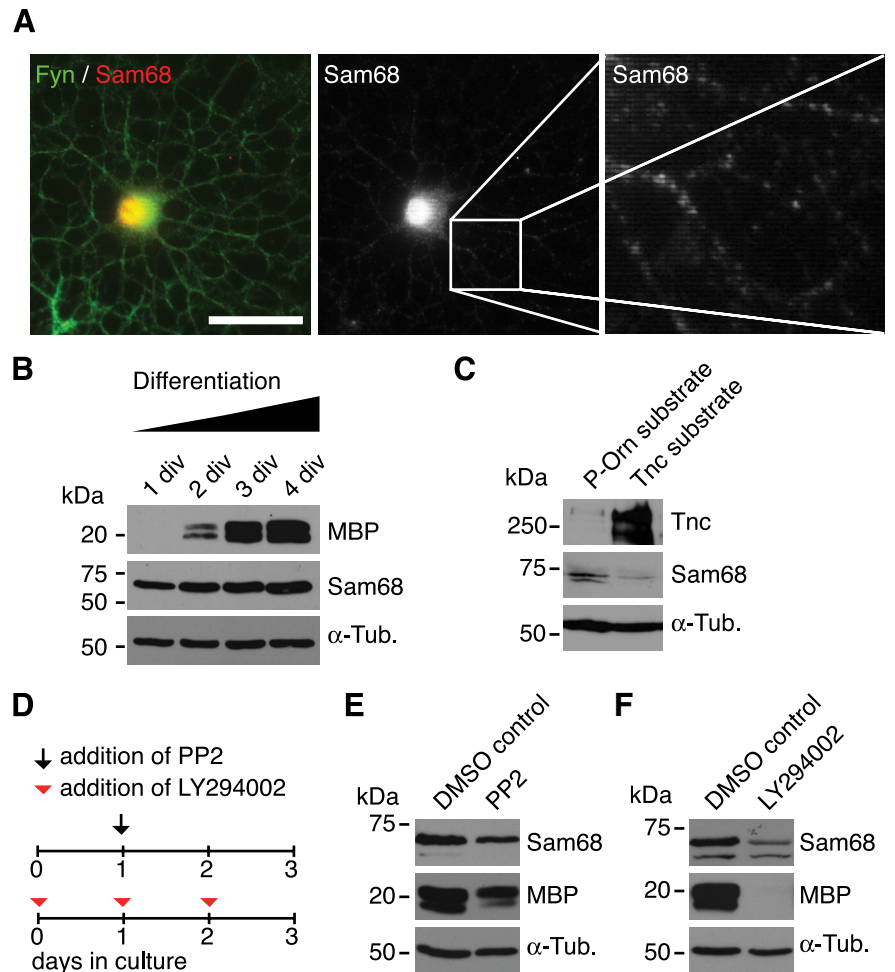


**Figure 7.** Sam68 expression increases with oligodendrocyte differentiation and is repressed through Tnc and inhibitors of SFK and PI3K. **A**, A Fyn-expressing oligodendrocyte coexpresses Sam68 protein. Most Sam68 immunoreactivity is restricted to the nucleus, although cytosolic Sam68 is also detectable. **B**, Immunoblotting of differentiating OPC cultures lysed after various cultivation periods showing that Sam68 at all stages of oligodendrocyte differentiation. Note, however, that Sam68 levels increase with differentiation (defined by increasing MBP levels). **C**, Immunoblotting of oligodendrocytes cultured on P-Orn or Tnc substrate for 24 h reveal that cultivation on Tnc reduces Sam68 expression levels. **D**, Schematic drawing of the cultivation protocol used for addition of PP2 or LY294002. **E**, **F**, Immunoblotting shows that oligodendrocytes display lower Sam68 expression levels in the presence of the SFK inhibitor PP2 or the PI3K inhibitor LY294002. Tubulin served as a loading control. Also note that the Sam68 antibody yielded one (**B**) or two bands (**C**, **E**, **F**), depending on which Sam68 antibody was used (see Materials and Methods). Scale bar, 50  $\mu$ m.

initiator of PI3K signaling (Sanchez-Margalet and Najib, 1999). As a mechanism by which changing levels of Sam68 in response to Tnc might regulate oligodendrocyte differentiation, therefore, one might predict that it intervenes in the pathways affected by the SFK inhibitor PP2 or the PI3K inhibitor LY294002. Indeed, when Sam68 was overexpressed, the inhibitory effect of PP2 on MBP expression was rescued (Fig. 8F). In contrast to this result, however, the LY294002-induced reduction of MBP expression appeared unaltered under these conditions (Fig. 8G). These results place Sam68 downstream of Fyn and parallel or upstream of the PI3K signaling pathway.

## Discussion

Several reports have pointed out that the ECM inhibits regeneration and suppresses plasticity in the adult CNS (Berardi et al., 2004; Fitch and Silver, 2008; Gervasi et al., 2008). By comparison, the role of the ECM in the stem and precursor cell microenvironment remains obscure, although the cellular microenvironment is crucial for stem cell maintenance and self-renewal (Scadden,

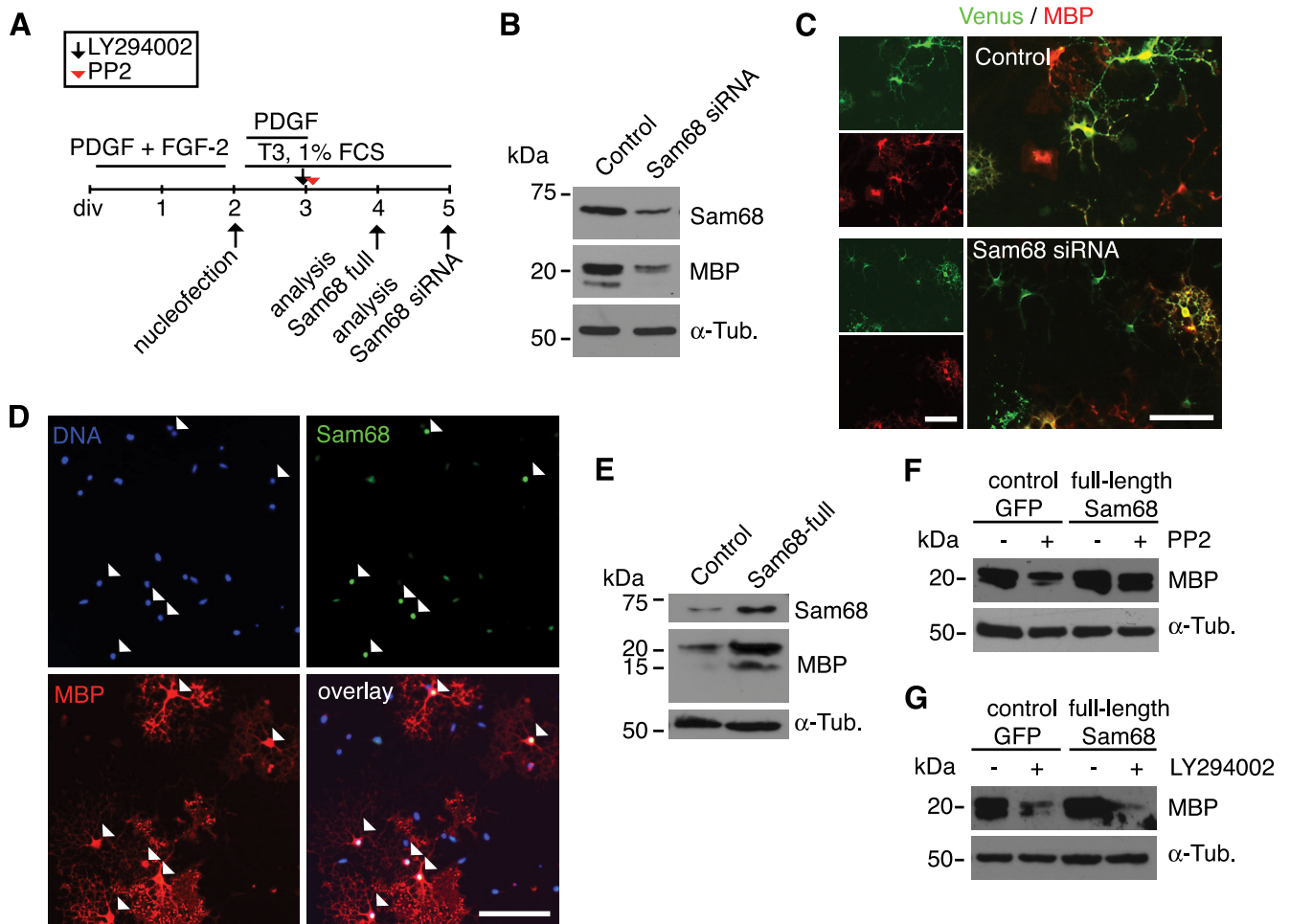


**Figure 8.** Sam68 promotes MBP expression in an SFK-dependent but not PI3K-dependent manner. **A**, The scheme describes the cultivation protocol used for knockdown or overexpression of Sam68. OPCs were expanded in the OPC expansion phase (PDGF + FGF-2) and differentiated after transfection by adding T3 + 1%FCS. Pharmacological inhibitors were applied when indicated. **B**, Immunoblotting shows a prominent decrease in Sam68 and also of MBP levels after transfection with Sam68 siRNA. **C**, Immunostaining for MBP showing that, in contrast to control cells, many transfected cells (Venus-positive) do not coexpress MBP after Sam68 knockdown. The quantitative numbers are given in the text. **D**, Immunocytochemical staining for Sam68 and MBP reveals that after transfection of a Sam68 full-length plasmid, most of the Sam68<sup>high</sup>-expressing cells coexpress MBP (arrowheads). The quantitative numbers are given in the text. **E**, Immunoblotting showing increased expression levels of MBP upon transfection with a Sam68 full-length plasmid. **F**, **G**, Immunoblottings showing that PP2-dependent reduction (**F**) but not LY294002-dependent reduction (**G**) of MBP expression is overcome by overexpressing Sam68. Scale bars, 100  $\mu$ m.

2006). Focusing on OPCs as a model, we reveal an inhibitory function of the ECM glycoprotein Tnc on differentiation and disentangle molecular details of ECM pathways designed to suppress the differentiation of a committed neural precursor cell. We show that Tnc suppresses the expression of MBP in oligodendrocytes both *in vitro* and *in vivo* during postnatal forebrain development, confirming its biological significance. The underlying signaling cascade requires the cell surface receptor Cntn1 and the associated Fyn kinase, and involves the regulation of the signaling adaptor and splice regulator Sam68. We further document that Akt signaling is diminished on Tnc substrates, an effect independent of the growth factors PDGF, EGF, or neuregulin-1 that are also important regulators of the oligodendrocyte lineage (Baron et al., 2005).

Elimination of Tnc in mice affects cells of the oligodendrocyte lineage at the different stages of proliferation, migration, survival, and differentiation (Kiernan et al., 1996; Garcion et al., 2001; Garwood et al., 2004; Czopka et al., 2009b). Similar to the role of other ECM molecules such as vitronectin, Tnc sensitizes OPCs for PDGF-regulated proliferation and survival at physiological concentrations of the growth factor in culture in an  $\alpha_v\beta_3$  integrin-dependent manner (Garcion et al., 2001; Baron et al.,

2002). In contrast to the processes operating in proliferation and survival, the mechanism(s) and signaling pathways that are engaged by Tnc to regulate differentiation are poorly understood. In the present study, we provide evidence that the regulation of MBP expression by Tnc involves lipid rafts, with Tnc and Cntn1 located on the extracellular face leading to Fyn activation on the cytosolic face of the plasma membrane. Tnc has previously been associated with lipid rafts in brain extracts (Kappler et al., 2002) and the alternatively spliced fibronectin type III domains TNfnBD directly interact with Cntn1, which results in neurite growth promotion in neurons (Rigato et al., 2002). However, our description of the functional consequence of a binding of Tnc to its receptor Cntn1 in a cellular context is novel. Cntn1 has previously been described as a functional ligand for Notch that regulates oligodendrocyte maturation (Hu et al., 2003). The Cntn1-to-Notch interaction revealed in that study occurred, however, in a *trans*-orientation. This differs significantly from the *cis*-acting mechanism for Tnc and Cntn1 demonstrated in our study. Moreover, Notch was not detected in lipid rafts (Hu et al., 2003). It is still conceivable that Tnc antagonizes interactions between Cntn1 and Notch in *trans*, under

the assumption that the Cntn1 affinity to Tnc is higher than that to Notch, but this remains a subject of speculation.

The interaction between Tnc and Cntn1 controls Fyn activity through increased phosphorylation of its regulatory Y531, which renders the kinase inactive. In this way, Tnc counteracts laminin-2, which induces the activation of Fyn by dephosphorylation of Y531 and drives oligodendrocyte differentiation (Colognato et al., 2004). Furthermore, Fyn regulates MBP expression and myelination in response to L1-CAM (White et al., 2008; Laursen et al., 2009). Therefore, we propose that the topologically specified enrichment of Tnc in OPCs and immature oligodendrocytes antagonizes the differentiation promoting activities of Fyn. How precisely this may occur is subject to speculation, but differential lipid raft composition and/or competing interactions between Tnc and CAMs of the Ig superfamily may play a role. Alternatively, as Cntn1 forms a complex with integrins in oligodendrocytes (Laursen et al., 2009), the activation of distinct integrin receptors and/or coupling to different intracellular signaling pathways could be involved, as has been proposed to explain the changes in the response of oligodendrocytes to PDGF as differentiation proceeds (Baron et al., 2005).

While the link among Tnc, Cntn1, and Fyn is established by our present work, the mechanisms involved in the Tnc-mediated reduction of Akt phosphorylation also reported in this study remains elusive. Our finding that PI3K inhibitors block oligodendrocyte differentiation without affecting survival when used at low concentrations is in line with the phenotype of transgenic mice that overexpress a constitutively active form of Akt in oligodendrocytes. Contrary to the predictions, these animals did not display alterations in cell survival but were hypermyelinated instead (Flores et al., 2008). Our observations are also in accordance with the observation that signaling from integrin-linked kinase to PI3K is required for myelin sheet formation and does not affect survival (Chun et al., 2003). Different groups recently revealed that mTOR (mammalian target of rapamycin) is an essential downstream target of Akt to regulate oligodendrocyte differentiation (Narayanan et al., 2009; Tyler et al., 2009). Our work identifies Tnc as a novel upstream regulator for Akt. However, a unique receptor that also acts upstream (and may therefore interact directly or indirectly with Tnc) has to our knowledge not yet been identified. It is tempting to speculate that the insulin receptor that signals via Akt and Src to control survival may be involved (Cui et al., 2005), as OPCs respond to IGF-1 (Barres et al., 1993) and the chemically defined media used contains high levels of insulin. Moreover, IGF-1 is an indispensable factor for oligodendrocyte differentiation and myelin production *in vitro* and *in vivo* since IGF receptor-deficient mice are hypomyelinated (Ye et al., 2002; Zeger et al., 2007). Interestingly, though, the inhibitory influence of Tnc on OPC differentiation appeared not to involve any interaction with the PDGF or neuregulin-1 pathways.

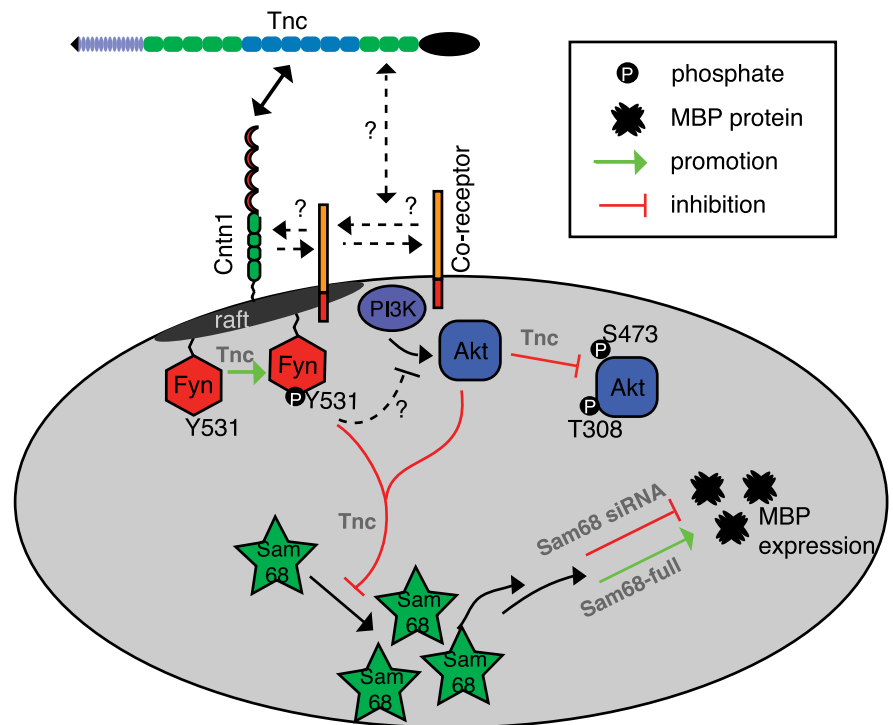


**Figure 9.** Proposed model of Tnc signaling in oligodendrocytes. The model summarizes the results obtained from the present study. We propose that Tnc binds Cntn1 within lipid rafts of oligodendrocyte membranes. This complex formation results in increased phosphorylation of the regulatory tyrosine 531 of Fyn, which reduces Fyn activity. Concomitantly, Tnc stimulation impairs phosphorylation of Akt through an as-yet-unidentified receptor. Tnc, impaired Fyn, and/or Akt activation prevents increased gene expression levels of Sam68, which are necessary for effective differentiation. It remains unknown whether Tnc prevents the activation of one linear or several parallel signaling cascades via binding to additional receptors and/or by regulation of clustering of multiple receptors within the plasma membrane.

In addition to Cntn1, Fyn, and Akt, we identified Sam68 as another molecule involved in Tnc signaling in oligodendrocytes as Tnc either directly or indirectly represses Sam68 protein levels in oligodendrocytes, similar to the situation in neural stem cells (Moritz et al., 2008). Sam68 has not been previously been implicated in oligodendrocyte differentiation, but this proposed function of Sam68 as a prodifferentiation molecules in neural cells is in line with the recent finding that overexpression of Sam68 in P19 cells increased the proportion of newly generated neurons (Chawla et al., 2009) and with our finding that overexpression in OPCs increased differentiation behavior. By what mechanism could Sam68 increase differentiation of oligodendrocytes? Sam68 can act as a signaling adaptor as well as a regulator of RNA splicing and stabilization (Lukong and Richard, 2003). Our work revealed that the inhibition of MBP expression by the Src kinase inhibitor PP2 could be overcome by overexpression of Sam68, whereas PI3K inhibition by LY294002 could not be rescued. In keeping with an interpretation of these results that Sam68 acts as a signaling adaptor upstream of Akt and downstream of Fyn in a prodifferentiation pathway, Sam68 is a tyrosine phosphorylation substrate of Fyn in T lymphocytes (Lang et al., 1999) and an initiator the PI3K pathway when phosphorylated by the insulin receptor (Sanchez-Margalet and Najib, 1999). In addition to these possible roles of Sam68 as a signal adapter, Sam68 is also a regulator of RNA metabolism (Lukong and Richard, 2003), so it is also possible that Sam68 promotes oligodendrocyte differentiation through its RNA-binding properties. This has previously been shown for other RNA-binding proteins like quaking (Larocque et al., 2002; Lukong and Richard, 2003) and heteroge-

neous nuclear ribonucleoprotein A2 (White et al., 2008). However, tyrosine phosphorylation of Sam68 negatively interferes with the RNA-binding properties of Sam68 (Lukong and Richard, 2003), so further studies are required to determine the balance of signal transduction or RNA binding in the role of Sam68.

Our data suggest that Cntn1 and Fyn are constituents of a preassembled lipid raft that functions as a differentiation-promoting signaling platform, which is maintained in an inactive state by the interaction between Tnc and Cntn1. This is consistent with current models of oligodendrocyte differentiation and has been schematized as a proposed model (Fig. 9). Although it remains to be seen whether Tnc regulates the signaling adapter and RNA-binding protein Sam68 directly via Fyn or through alternative pathways and how Sam68 promotes oligodendrocyte differentiation in detail, the identification of Sam68 as a Tnc and Fyn target in oligodendrocytes extends our understanding of the ECM-dependent signaling cascades by linking plasma membrane signaling domains to regulation of RNA metabolism.

## References

- Back SA, Tuohy TM, Chen H, Wallingford N, Craig A, Struve J, Luo NL, Banine F, Liu Y, Chang A, Trapp BD, Bebo BF Jr, Rao MS, Sherman LS (2005) Hyaluronan accumulates in demyelinated lesions and inhibits oligodendrocyte progenitor maturation. *Nat Med* 11:966–972.
- Baron W, Shattil SJ, ffrench-Constant C (2002) The oligodendrocyte precursor mitogen PDGF stimulates proliferation by activation of alpha(v)-beta3 integrins. *EMBO J* 21:1957–1966.
- Baron W, Colognato H, ffrench-Constant C (2005) Integrin-growth factor interactions as regulators of oligodendroglial development and function. *Glia* 49:467–479.
- Barres BA, Schmid R, Sendtner M, Raff MC (1993) Multiple extracellular signals are required for long-term oligodendrocyte survival. *Development* 118:283–295.
- Berardi N, Pizzorusso T, Maffei L (2004) Extracellular matrix and visual cortical plasticity: freeing the synapse. *Neuron* 44:905–908.
- Chawla G, Lin CH, Han A, Shiue L, Ares M Jr, Black DL (2009) Sam68 regulates a set of alternatively spliced exons during neurogenesis. *Mol Cell Biol* 29:201–213.
- Chun SJ, Rasband MN, Sidman RL, Habib AA, Vartanian T (2003) Integrin-linked kinase is required for laminin-2-induced oligodendrocyte cell spreading and CNS myelination. *J Cell Biol* 163:397–408.
- Colognato H, Baron W, Avellana-Adalid V, Relvas JB, Baron-Van Evercooren A, Georges-Labouesse E, ffrench-Constant C (2002) CNS integrin switch growth factor signalling to promote target-dependent survival. *Nat Cell Biol* 4:833–841.
- Colognato H, Ramachandrapa S, Olsen IM, ffrench-Constant C (2004) Integrins direct Src family kinases to regulate distinct phases of oligodendrocyte development. *J Cell Biol* 167:365–375.
- Cui QL, Zheng WH, Quirion R, Almazan G (2005) Inhibition of Src-like kinases reveals Akt-dependent and -independent pathways in insulin-like growth factor I-mediated oligodendrocyte progenitor survival. *J Biol Chem* 280:8918–8928.
- Czopka T, Hennen E, von Holst A, Faissner A (2009a) Novel conserved oligodendrocyte surface epitope identified by monoclonal antibody 4860. *Cell Tissue Res* 338:161–170.
- Czopka T, Von Holst A, Schmidt G, ffrench-Constant C, Faissner A (2009b) Tenascin C and tenascin R similarly prevent the formation of myelin membranes in a RhoA-dependent manner, but antagonistically regulate the expression of myelin basic protein via a separate pathway. *Glia* 57:1790–1801.
- Decker L, ffrench-Constant C (2004) Lipid rafts and integrin activation regulate oligodendrocyte survival. *J Neurosci* 24:3816–3825.
- Faissner A, Kruse J (1990) J1/tenascin is a repulsive substrate for central nervous system neurons. *Neuron* 5:627–637.
- Falk J, Bonnon C, Girault JA, Faivre-Sarrailh C (2002) F3/contactin, a neuronal cell adhesion molecule implicated in axogenesis and myelination. *Biol Cell* 94:327–334.
- Fitch MT, Silver J (2008) CNS injury, glial scars, and inflammation: inhibitory extracellular matrices and regeneration failure. *Exp Neurol* 209:294–301.
- Flores AI, Mallon BS, Matsui T, Ogawa W, Rosenzweig A, Okamoto T, Macklin WB (2000) Akt-mediated survival of oligodendrocytes induced by neurotrophins. *J Neurosci* 20:7622–7630.
- Flores AI, Narayanan SP, Morse EN, Shick HE, Yin X, Kidd G, Avila RL, Kirschner DA, Macklin WB (2008) Constitutively active Akt induces enhanced myelination in the CNS. *J Neurosci* 28:7174–7183.
- Forsberg E, Hirsch E, Fröhlich L, Meyer M, Ekblom P, Aszodi A, Werner S, Fässler R (1996) Skin wounds and severed nerves heal normally in mice lacking tenascin-C. *Proc Natl Acad Sci U S A* 93:6594–6599.
- Garcion E, Faissner A, ffrench-Constant C (2001) Knockout mice reveal a contribution of the extracellular matrix molecule tenascin-C to neural precursor proliferation and migration. *Development* 128:2485–2496.
- Garwood J, Garcion E, Dobbertin A, Heck N, Calco V, ffrench-Constant C, Faissner A (2004) The extracellular matrix glycoprotein tenascin-C is expressed by oligodendrocyte precursor cells and required for the regulation of maturation rate, survival and responsiveness to platelet-derived growth factor. *Eur J Neurosci* 20:2524–2540.
- Gervasi NM, Kwok JC, Fawcett JW (2008) Role of extracellular factors in axon regeneration in the CNS: implications for therapy. *Regen Med* 3:907–923.
- Gielen E, Baron W, Vandeven M, Steels P, Hoekstra D, Ameloot M (2006) Rafts in oligodendrocytes: evidence and structure-function relationship. *Glia* 54:499–512.
- Grange J, Boyer V, Fabian-Fine R, Fredj NB, Sadoul R, Goldberg Y (2004) Somatodendritic localization and mRNA association of the splicing regulatory protein Sam68 in the hippocampus and cortex. *J Neurosci Res* 75:654–666.
- Hu QD, Ang BT, Karsak M, Hu WP, Cui XY, Duka T, Takeda Y, Chia W, Sankar N, Ng YK, Ling EA, Maciag T, Small D, Trifonova R, Kopan R, Okano H, Nakafuku M, Chiba S, Hirai H, Aster JC, et al (2003) F3/contactin acts as a functional ligand for Notch during oligodendrocyte maturation. *Cell* 115:163–175.
- Huot ME, Brown CM, Lamarche-Vane N, Richard S (2009) An adaptor role for cytoplasmic Sam68 in modulating Src activity during cell polarization. *Mol Cell Biol* 29:1933–1943.
- Hutchinson J, Jin J, Cardiff RD, Woodgett JR, Muller WJ (2001) Activation of Akt (protein kinase B) in mammary epithelium provides a critical cell survival signal required for tumor progression. *Mol Cell Biol* 21:2203–2212.
- Joester A, Faissner A (2001) The structure and function of tenascins in the nervous system. *Matrix Biol* 20:13–22.
- Kappler J, Baader SL, Franken S, Pesheva P, Schilling K, Rauch U, Gieselmann V (2002) Tenascins are associated with lipid rafts isolated from mouse brain. *Biochem Biophys Res Commun* 294:742–747.
- Keilhauer G, Faissner A, Schachner M (1985) Differential inhibition of neurone-neurone, neurone-astrocyte and astrocyte-astrocyte adhesion by L1, L2 and N-CAM antibodies. *Nature* 316:728–730.
- Kiernan BW, Götz B, Faissner A, ffrench-Constant C (1996) Tenascin-C inhibits oligodendrocyte precursor cell migration by both adhesion-dependent and adhesion-independent mechanisms. *Mol Cell Neurosci* 7:322–335.
- Krämer EM, Klein C, Koch T, Boytinch M, Trotter J (1999) Compartmentation of Fyn kinase with glycosylphosphatidylinositol-anchored molecules in oligodendrocytes facilitates kinase activation during myelination. *J Biol Chem* 274:29042–29049.
- Lang V, Semichon M, Michel F, Brossard C, Gary-Gouy H, Bismuth G (1999) Fyn membrane localization is necessary to induce the constitutive tyrosine phosphorylation of Sam68 in the nucleus of T lymphocytes. *J Immunol* 162:7224–7232.
- Larocque D, Richard S (2005) QUAKING KH domain proteins as regulators of glial cell fate and myelination. *RNA Biol* 2:37–40.
- Larocque D, Pilotte J, Chen T, Cloutier F, Massie B, Pedraza L, Couture R, Lasko P, Almazan G, Richard S (2002) Nuclear retention of MBP mRNAs in the quaking viable mice. *Neuron* 36:815–829.
- Laursen LS, Chan CW, ffrench-Constant C (2009) An integrin-contactin complex regulates CNS myelination by differential Fyn phosphorylation. *J Neurosci* 29:9174–9185.
- Lu Z, Ku L, Chen Y, Feng Y (2005) Developmental abnormalities of myelin basic protein expression in fyn knock-out brain reveal a role of Fyn in posttranscriptional regulation. *J Biol Chem* 280:389–395.
- Lukong KE, Richard S (2003) Sam68, the KH domain-containing superSTAR. *Biochim Biophys Acta* 1653:73–86.

- Matter N, Herrlich P, König H (2002) Signal-dependent regulation of splicing via phosphorylation of Sam68. *Nature* 420:691–695.
- McCarthy KD, de Vellis J (1980) Preparation of separate astroglial and oligodendroglial cell cultures from rat cerebral tissue. *J Cell Biol* 85:890–902.
- Milner R, Ffrench-Constant C (1994) A developmental analysis of oligodendroglial integrins in primary cells: changes in alpha v-associated beta subunits during differentiation. *Development* 120:3497–3506.
- Moritz S, Lehmann S, Faissner A, von Holst A (2008) An induction gene trap screen in neural stem cells reveals an instructive function of the niche and identifies the splicing regulator sam68 as a tenascin-C-regulated target gene. *Stem Cells* 26:2321–2331.
- Nagai T, Ibata K, Park ES, Kubota M, Mikoshiba K, Miyawaki A (2002) A variant of yellow fluorescent protein with fast and efficient maturation for cell-biological applications. *Nat Biotechnol* 20:87–90.
- Narayanan SP, Flores AI, Wang F, Macklin WB (2009) Akt signals through the mammalian target of rapamycin pathway to regulate CNS myelination. *J Neurosci* 29:6860–6870.
- Osterhout DJ, Wolven A, Wolf RM, Resh MD, Chao MV (1999) Morphological differentiation of oligodendrocytes requires activation of Fyn tyrosine kinase. *J Cell Biol* 145:1209–1218.
- Paronetto MP, Achsel T, Massiello A, Chalfant CE, Sette C (2007) The RNA-binding protein Sam68 modulates the alternative splicing of Bcl-x. *J Cell Biol* 176:929–939.
- Pringle NP, Yu WP, Guthrie S, Roelink H, Lumsden A, Peterson AC, Richardson WD (1996) Determination of neuroepithelial cell fate: induction of the oligodendrocyte lineage by ventral midline cells and sonic hedgehog. *Dev Biol* 177:30–42.
- Rhee JM, Purity MK, Lackan CS, Long JZ, Kondoh G, Takeda J, Hadjantonakis AK (2006) In vivo imaging and differential localization of lipid-modified GFP-variant fusions in embryonic stem cells and mice. *Genesis* 44:202–218.
- Rigato F, Garwood J, Calco V, Heck N, Faivre-Sarrailh C, Faissner A (2002) Tenascin-C promotes neurite outgrowth of embryonic hippocampal neurons through the alternatively spliced fibronectin type III BD domains via activation of the cell adhesion molecule F3/contactin. *J Neurosci* 22:6596–6609.
- Sánchez-Margalet V, Najib S (1999) p68 Sam is a substrate of the insulin receptor and associates with the SH2 domains of p85 PI3K. *FEBS Lett* 455:307–310.
- Scadden DT (2006) The stem-cell niche as an entity of action. *Nature* 441:1075–1079.
- Sommer I, Schachner M (1981) Monoclonal antibodies (O1 to O4) to oligodendrocyte cell surfaces: an immunocytological study in the central nervous system. *Dev Biol* 83:311–327.
- Sperber BR, Boyle-Walsh EA, Engleka MJ, Gadue P, Peterson AC, Stein PL, Scherer SS, McMorris FA (2001) A unique role for Fyn in CNS myelination. *J Neurosci* 21:2039–2047.
- Stolt CC, Rehberg S, Ader M, Lommes P, Riethmacher D, Schachner M, Bartsch U, Wegner M (2002) Terminal differentiation of myelin-forming oligodendrocytes depends on the transcription factor Sox10. *Genes Dev* 16:165–170.
- Talts JF, Wirl G, Dictor M, Muller WJ, Fässler R (1999) Tenascin-C modulates tumor stroma and monocyte/macrophage recruitment but not tumor growth or metastasis in a mouse strain with spontaneous mammary cancer. *J Cell Sci* 112:1855–1864.
- Tyler WA, Gangoli N, Gokina P, Kim HA, Covey M, Levison SW, Wood TL (2009) Activation of the mammalian target of rapamycin (mTOR) is essential for oligodendrocyte differentiation. *J Neurosci* 29:6367–6378.
- Umemori H, Sato S, Yagi T, Aizawa S, Yamamoto T (1994) Initial events of myelination involve Fyn tyrosine kinase signalling. *Nature* 367:572–576.
- von Holst A, Sirko S, Faissner A (2006) The unique 473HD-Chondroitinsulfate epitope is expressed by radial glia and involved in neural precursor cell proliferation. *J Neurosci* 26:4082–4094.
- White R, Gonsior C, Krämer-Albers EM, Stöhr N, Hüttelmaier S, Trotter J (2008) Activation of oligodendroglial Fyn kinase enhances translation of mRNAs transported in hnRNP A2-dependent RNA granules. *J Cell Biol* 181:579–586.
- Ye P, Li L, Richards RG, DiAugustine RP, D'Ercole AJ (2002) Myelination is altered in insulin-like growth factor-I null mutant mice. *J Neurosci* 22:6041–6051.
- Zacharias U, Nörenberg U, Rathjen FG (1999) Functional interactions of the immunoglobulin superfamily member F11 are differentially regulated by the extracellular matrix proteins tenascin-R and tenascin-C. *J Biol Chem* 274:24357–24365.
- Zeger M, Popken G, Zhang J, Xuan S, Lu QR, Schwab MH, Nave KA, Rowitch D, D'Ercole AJ, Ye P (2007) Insulin-like growth factor type 1 receptor signaling in the cells of oligodendrocyte lineage is required for normal in vivo oligodendrocyte development and myelination. *Glia* 55:400–411.